

Published in final edited form as:

*Burns*. 2008 December ; 34(8): 1119–1127. doi:10.1016/j.burns.2008.03.013.

## A porcine model of full-thickness burn, excision and skin autografting

Ludwik K. Branski<sup>a,1</sup>, Rainer Mittermayr<sup>b,1</sup>, David N. Herndon<sup>a</sup>, William B. Norbury<sup>a</sup>, Oscar E. Masters<sup>a</sup>, Martina Hofmann<sup>b</sup>, Daniel L. Traber<sup>a</sup>, Heinz Redl<sup>b</sup>, and Marc G. Jeschke<sup>a,\*</sup>

*a*Shriners Hospital for Children and University of Texas Medical Branch, Galveston, TX, United States

*b*Research Center of the AUVA, Ludwig Boltzmann Institute for Experimental and Clinical Traumatology, Vienna, Austria

### Abstract

Acute burn wounds often require early excision and adequate coverage to prevent further hypothermia, protein and fluid losses, and the risk of infection. Meshed autologous skin grafts are generally regarded as the standard treatment for extensive full-thickness burns. Graft take and rate of wound healing, however, depend on several endogenous factors. This paper describes a standardized reproducible porcine model of burn and skin grafting which can be used to study the effects of topical treatments on graft take and re-epithelialization.

Procedures provide a protocol for successful porcine burn wound experiments with special focus on pre-operative care, anesthesia, burn allocation, excision and grafting, postoperative treatment, dressing application, and specimen collection. Selected outcome measurements include percent area of wound closure by planimetry, wound assessment using a clinical assessment scale, and histological scoring.

The use of this standardized model provides burn researchers with a valuable tool for the comparison of different topical drug treatments and dressing materials in a setting that closely mimics clinical reality.

### Keywords

Burn; Burn excision; Wound healing; Reconstruction; Autograft

## 1. Background

Standard treatment for severe burns currently includes early excision and adequate coverage to prevent hypothermia, protein and fluid loss, and risk of exogenous infection [1]. Autologous meshed split-thickness skin grafts are generally regarded as the standard treatment for extensive full-thickness burns. Early wound healing with concomitant wound closure is a major factor in patient outcome and infection control.

To determine new treatment options which enhance and accelerate wound healing, many investigators rely on animal models to closely observe the healing process. Many animal models have been described in the literature, mostly involving rodents and pigs, with different

\*Corresponding author. Tel.: +1 409 770 6742; fax: +1409 770 6919. E-mail address: majeschk@utmb.edu (M.G. Jeschke).

<sup>1</sup>Authors contributed equally to this manuscript.

**Conflict of interest statement** None of the authors have disclosed any conflict of interest associated with this manuscript.

burn depths, sizes, and mechanisms [2-6]. However, there has been no large animal model described which would encompass a burn excision and autografting, for an extended observation of over 2 weeks, to closely monitor the wound healing progress and its mechanisms. This paper presents a porcine model for the assessment of multiple treatments and quantification of differences in burn wound healing.

## 2. Procedures

### 2.1. Basic and study guidelines

Pigs have been used as models for wound healing studies due to their structural and functional resemblance to human skin. The thickness of porcine skin differs greatly depending on the location (pig epidermis: 30–140  $\mu\text{m}$ ; Human epidermis: 50–120  $\mu\text{m}$ ) [7]. Further, the vascularization of human and porcine skin is similar [8], with both human and pig having about 95% collagen and 2% elastic fibers in their extracellular matrix. This composition presents similar elastic components which is paramount in wound contraction [9]. Both pig and human skin have sparse body hair and do not re-epithelialize as rapidly as rodents with high amounts of adnexal structures [6]. Porcine skin has a similar epidermal turnover time, type of keratins and stratum corneum thickness when compared to human skin [10,11]. The pig model also allows many comparisons of local treatments on the same animal with reasonably sized treatment sites.

Porcine research is labor and cost intensive with numerous logistic and ethical requirements. At our institute, all experiments were conducted in a central large animal research facility. Class A (40–65 kg) Yorkshire pigs were purchased from a single breeding farm and, after arrival, housed individually at the animal resource center for at least 1 week for acclimatization. Pigs were then transferred to our laboratory and housed in individual cages of approximately 3 m<sup>2</sup> throughout the experiment. They received a standard porcine diet (LabDiet® 5084, PMI Nutrition, IN) once daily and water *ad libitum*. All pigs were fasted overnight before any experimental procedure. Housing and animal care were provided according to the National Research Council guidelines [12]. Animals were tended by the investigators and continuously monitored by trained personnel. The ability to quickly recognize and correct problems, such as dressing failures, postoperative bleeding, or excessive pain, was required for a successful wound healing study.

The pig model was specifically developed to observe wound healing after a full-thickness burn, wound excision, and skin grafting. Twenty-four hours after receiving a full-thickness burn, pigs were returned to the operating room for burn excision and overlay with meshed skin autograft. Dressing changes were made at days 2, 5, and 9 after grafting, with all pigs sacrificed at day 14. Times for dressing changes were selected to compensate for the initially higher rate of exudation, with dressing change intervals increasing from 2 days at the beginning to 5 days at the end of the experiment. Burn wound biopsies were taken at day 14. Small punch biopsies of 3.5 mm diameter could be obtained during each dressing change.

### 2.2. Anesthesia, pre- and postoperative care

The choice of appropriate methods for sedation, induction of anesthesia, and pain control was of vital importance throughout the entire experiment. To avoid vomiting and aspiration, all animals were fasted overnight. Anesthesia was induced by an intramuscular injection of 0.04 ml/kg TKX (1 ml TKX contains 0.5 mg Ketanest (Ketaset™, Wyeth Inc., NJ), 0.5 mg Xylazine (Tranquived™, Vedco Inc., MO), and 1 mg Telamine/Zolazepam (Telazol™, Wyeth Inc., NJ)). This mixture was used for its quick onset of anesthesia and the duration of sedation which allowed safe transportation to the preparation room. Usually, animals were sufficiently sedated 5–15 min after injection. Prior to any surgical intervention, pigs were weighed and clipped

with an electric clipper. This procedure was performed in a separate preparation room with the additional use of 2–3% of isoflurane in room air via face mask.

After preparation, pigs were transferred to the operating room, placed on an operating table in the prone position, pre-oxygenated with 100% oxygen via inhalation mask, and intubated with a straight laryngoscope blade using a number 7 or 8 endotracheal tube. After intubation, isoflurane was delivered as an oxygen:nitrous oxide mixture (2:1) to maintain anesthesia (Aestive® 5, Draeger Medical Inc., PA). Before the first procedure, animals were further depilated using a disposable razor blade. In contrast to previous reports [4,13] we did not observe skin infections due to use of razor blades.

Before each initial burn, a venous catheter was placed in the right jugular vein, tunneled underneath the skin of the lateral neck and released through the dorsal neck region. The catheter remained in place for the entire experiment and was used for repeated blood draws and infusion of fluids. Ringer's Lactate solution (5 ml/kg h) was used for intraoperative fluid needs.

Heart rate and oxygen saturation were monitored throughout the surgical procedure via ear oximeter. Body temperature was monitored with a rectal digital thermometer. To maintain a normal body core temperature during the excision and grafting procedure, a disposable Bear Hugger® blanket (Arizant Healthcare Inc., Eden Prairie, MN), set at 40 °C, was used.

After each procedure, animals were allowed to recover on the operating table with the temperature control blanket placed over the dressing. Once spontaneous breathing stabilized they were extubated and transferred back to their cage. To minimize postoperative shivering, temperature control was continued in the cage using Bair Hugger® blankets or a heat lamp.

Postoperative analgesia was provided with transdermal fentanyl patches (Duragesic® 25 or 100, Janssen Pharmaceuticals, NJ) applied on the dorsal neck behind the ear and kept in place using surgical staples and an additional protective layer of adhesive transparent dressing. Fentanyl patches proved to be effective in both pain control and the reduction of postoperative activity. Food intake remained stable with no weight loss. These observations were in concordance with previous literature [14–17] and were particularly important since successful long-term observation of wounds could only be achieved if dressings remained intact. The choice of transdermal morphine postoperative analgesia and a strict dressing regimen were two important factors that guaranteed successful completion of burn wound healing studies. With this protocol, the application of non-steroidal analgesics was practically eliminated.

Intravenous perioperative antimicrobial prophylaxis was provided. Cephalosporin (Cefazol® 1 g i.v., Bosch Pharmaceuticals, IN) was administered before each operation and dressing changes. Levofloxacin (Levaquin® 500 mg tablets p.o., Ortho-McNeil Pharmaceuticals, TX) was continued for 7 days after burn. With the use of this antimicrobial therapy, the overall wound infection rate was less than 5%.

### 2.3. Burn injury

Contact burns were applied paravertebrally under aseptic conditions. This was accomplished by placing a heated aluminum bar (custom-made at the Ludwig Boltzmann Institute, Vienna, Austria) on the dorsum of the animal. The aluminum bar was heated to 200 °C with a Meeker gas burner. The core temperature of the bar was monitored with a digital thermometer. The heated bar was placed on the animal for 30 s. Application pressure was measured with a 50 ml syringe attached to the aluminum bar via a heat insulation unit. This device was designed to exert a pressure of 0.4 kg/cm<sup>2</sup> when the piston was pushed into the barrel of the syringe with one hand from the “20 ml” to the “10 ml” mark, while the other hand was holding the heat insulation unit to prevent any additional pressure on the heat transfer bar (Fig. 1).

Burn sites of approximately 40 cm<sup>2</sup> each were made on the dorsum of the animal with 4 cm between each site or from the spine. The total burn size did not exceed 15% of the entire body surface area.

In the initial experiments, biopsies of burned tissue were obtained at 24 h, 48 h, and 7 days after burn to assess the depth of the burn under experimental conditions. Skin biopsies from the burn sites were stained with Hematoxylin and Eosin and with Masson's trichrome to determine the extent of burn as determined by the depth of collagen degeneration (Fig. 2). Using the burn procedure as described achieved the complete coagulation of the superficial and most of the deep collagenous structures. The underlying skeletal musculature was affected by the burn, causing compression of fasciculi and some loss of fibres, but no overall necrosis (Fig. 2). Interestingly, no progression of burn depth at 7 days postburn compared to the early timepoints was noted. Concomitant with the burn itself was a zone of stasis and hyperemia in the surrounding tissue.

During and just after the burn procedure, all pigs were resuscitated with Ringer's Lactate solution at a rate of 10 ml/kg h, usually reaching a total intravenous resuscitation volume of 20 ml/kg. The animals then had free access to water.

#### 2.4. Excision and grafting

To mimic the clinical situation in burned patients, the burn was excised to the level of the underlying muscular fascia 24 h after the injury. The average total size of the resulting defect was approximately 50 cm<sup>2</sup>. For autograft harvesting, the distal dorsum and hind quarters of the animal were used. Prior to graft harvesting, the skin was lubricated with vaseline-impregnated gauze to facilitate the operation of an electric Padgett dermatome (Integra Lifesciences Inc., Plainsboro, NJ). Split-thickness skin grafts (0.4mm thickness) were harvested and placed between saline-soaked gauze swabs. Directly prior to their application on the prepared wounds, grafts were meshed to 1:3 ratio and trimmed to the size of the wounds.

Autografts were fixed with skin staples using a disposable skin stapler or with a two-component fibrin sealant [18].

#### 2.5. Dressing application

To protect the wounds from outside contamination and infection a multi-layer dressing, which could withstand the natural tendency of pigs to repeatedly scratch their back, was used. Each dressing change was made during full anesthesia. Intubation was the preferred method, but mask anesthesia could be used for quick dressing changes.

The first dressing layer, placed directly on the autograft, consisted of non-sticking (silicone) oil emulsion dressing. This dressing was covered with a thin protective layer of antimicrobial ointment consisting of 1% Nystatin and 2% Polymyxin B/Bacitracin in a Vaseline formulation. This preparation did not absorb wound fluid and thus protected grafts from detaching during dressing changes. The dressing was attached to each corner of the wound field with skin staples.

A second dressing layer of double polyurethane film, such as Opsite<sup>®</sup> (Smith&Nephew Inc., FL), was placed over the first dressing layer to seal off the wound fields while providing vapor permeability. We preferred the use of 20 cm × 40 cm or 40 cm × 60 cm sheets to cover the entire back of the animal. Application of Opsite<sup>®</sup> ensured that each individual wound field could be separated, thus avoiding cross-contamination when different treatments were used on adjacent wounds. The use of the second layer after day 5 usually led to hypergranulation and sporadic graft loss and, therefore, was limited to the initial dressing application and first dressing change.

The third level of coverage consisted of elastic bandage, such as VetRap® (3M Health Care, MN). This bandage exerted a mild pressure on the wound and kept skin autografts attached to the wound bed, but did not restrict breathing or movement. Three to five rolls of VetRap® were needed for each animal. This dressing was also wrapped around the front legs for a proper fit and to avoid dislocation. The pig was then covered with a stocking hose made out of cotton and elastic fibers, such as Goat tube® (Sullivan Supplies, Houston, TX), to provide protection against feces, urine, and water contamination (Fig. 3). This dressing regimen was well tolerated with total graft loss and infection minimized throughout the course of a study.

## 2.6. Specimen collection

To evaluate graft healing, skin specimens were taken from the center of the grafted area at day 14 as complete horizontal cross-sections of approximately 1 cm thickness. All biopsies were stored in 10% buffered formaldehyde solution for analysis.

## 3. Outcome measurements

### 3.1. Planimetric wound healing assessments

After the initial autografting and during each dressing change, standardized digital photographs of the wound fields were taken. A calibrated benchmark was positioned adjacent to each wound and photographs were taken at a right angle to the wound site (Fig. 4). Photographs were processed using planimetric software (Lucia G®, Version 4.8, Laboratory Imaging Ltd., Czech Republic). For each wound and each timepoint, total wound size and the sizes of all open mesh interstices were measured. To avoid human bias, investigators reading outcome measurements were blinded to group allocation. Total wound size reduction and open mesh interstices were presented as percentage of initial open wound size (Fig. 5). At the end of 2 weeks, a nearly complete wound closure was associated with an average contraction of about 25% of the initial wound size. Although the rate of wound closure in pigs was slower than in humans, especially slower than in burned children, closure and contraction rates were consistent throughout the experiments.

### 3.2. Clinical wound healing scores

Re-epithelialization, graft adherence, graft dislocation, occurrence of hypergranulation, hematoma, and fibrin deposition were graded using a scale ranging from 0 to 5 (Table 1). These scores were generated and recorded independently by two investigators during dressing changes. Hypergranulation and graft dislocation usually peaked at day 9, while fibrin deposition remained relatively high at days 5 and 9 (Fig. 6).

### 3.3. Wound histology

Wound specimens, taken 14 days after grafting, were embedded in paraffin, sectioned, and stained with Hematoxylin and Eosin. Measures of dermal and epidermal thickness used a Leica microscope with 200× magnification, high-resolution CCD camera digital picture capture, and image analysis software. The cross-sections were divided into healthy tissue, wound edge, and wound center. For each section, two random visual fields were chosen and three measurements of dermal and epidermal thickness were obtained. The final results for each section was a mean of 12 dermal and 12 epidermal measurements (Fig. 7). Two observers, blinded to treatment, made the measurements.

### 3.4. Hematology and cytokines

Hematologic parameters and selected serum cytokines were used to evaluate the general condition of the animal and to assess systemic effects of the burn. Blood samples were obtained prior to burns (baseline), before excision and grafting, and on days 2, 5, 9, and 14 after excision.

Hemoglobin, WBC, and Platelets were measured using a veterinary hematology analyzer (Drew-Scientific HemaVet 950, Escalon Medical Corp, PA). Values for IL-6 and TNF- $\alpha$  were measured by ELISA using specific porcine kits (P6000 Porcine IL-6 Quantikine Elisa Kit and PTA00 Porcine TNF- $\alpha$  Quantikine Elisa Kit, R&D Systems, Minneapolis, MN). Throughout the 2-week study, no animal showed clinical signs of bleeding or infection as confirmed by hematology parameters (Fig. 8). All values remained in the normal range for Yorkshire swine [19]. Levels of IL-6 and TNF- $\alpha$  were below the level of detection at all measurement times, indicating that although considerable injury was inflicted upon the animal, burn and donor sites could be handled without occurrence of systemic infections.

## 4. Discussion

Experiments on burn wound excision and skin autografting require a reliable model of full-thickness burn and subsequent fascial excision, which includes coverage with meshed autograft and permits an extended observation time of up to 14 days without notable systemic effects. In addition, the critical aspects of pain control and appropriate dressing application must be addressed.

Our model design was influenced by several other porcine burn models. Middelkoop et al. developed an excisional model for testing dermal and epidermal substitutes and for scald and contact burns [2] which favored a burn size of approximately 50 cm<sup>2</sup>. Several porcine burn models, detailed descriptions of burn depth and scar assessments, and dressing application methods have been published by Singer et al. [3-5,20,21]. Mittermayr et al. [22] developed a pig model of excision and grafting with non-meshed skin autograft and performed wound healing measurements for 2 weeks. We have combined several of these techniques to develop our pig model to study excision and autografting.

The frequency of dressing changes used in this model was a compromise between the clinical practice used in humans, where dressing changes on skin autografts are usually not performed for at least 4 days postoperatively, and experimental planning, where frequent observations in the early phase of graft healing are necessary to determine differences between treatments. The protocol developed in this study was also influenced by the general difficulty of maintaining a clean and tightly sealed dressing on an awake pig and the natural rate of wound exudation, which steadily decreased within the first 5–7 days. This study showed that three dressing changes until day 14 were most practical.

The model described in this paper has several limitations. Although biopsies of burned sites were performed at 24 h, 48 h, and 7 days after burn, we did not see relevant progression of burn depth over this period of time. It is worth noticing that another author showed a progression in burn depth over the course of up to 4 days [23]. The excision of the burn wound performed later than 24 h after burn might change the rate of graft take and wound healing pace, however, this variable was not investigated. Another limitation of this study involved specimens for histology which were not obtained until the last day of the study. Repeated skin biopsies for evaluation of wound healing in the pig model were first described by Winter [24]. This method has many advantages, as it allows the evaluation of re-epithelialization and the use of immunohistochemical methodology. We, however, chose to avoid disturbances in the wound healing process and a possible infection from multiple biopsies, and focused on the evaluation of the wound healing progress via planimetry.

This model was developed specifically for evaluating acute burn wounds, and not for evaluating long-term outcomes. The 14-day observation may not be sufficient to evaluate scarring mechanisms following different treatment protocols. For purposes of scar studies in the porcine model, the Red Duroc strain, which shows hypertrophic scarring after wounding, is the pig of



choice and has been used in wound healing for over 35 years [25-29]. The further evaluation of graft take and healing times should be performed on a model of tangential excision as opposed to the fascial excision used in this study. In a large human cohort study, the recipient bed has recently been found to play a minor role [30], however, no studies have been performed to test this finding in the porcine burn model.

## Acknowledgements

Financial support for this work came from the Clayton Foundation for Research, Houston, TX. Ludwik K. Branski and William B. Norbury are supported by research fellowship grants from the Shriners Hospitals for Children. The authors would like to acknowledge the large animal facility at the Shriners Hospital for Children and Lilian Traber, Thomas Miszkowski and John R. Salsbury, for their great support in conducting the animal studies. We also thank Zafar Khakpour, LBI Vienna, for the design and construction of the burn apparatus, and Pat Sellers of the Shriners Hospital Pathology core lab for the preparation of histological slides. We would also like to thank Dr. Melitta Bilban and Baxter AG, Vienna, Austria for their support of this study, and Dr. Robert E. Barrow for manuscript review.

## References

1. Herndon DN, Parks DH. Comparison of serial debridement and autografting and early massive excision with cadaver skin overlay in the treatment of large burns in children. *J Trauma* 1986;26(2):149–52. [PubMed: 3511266]
2. Middelkoop E, van den Bogaardt AJ, Lamme EN, Hoekstra MJ, Brandsma K, Ulrich MM. Porcine wound models for skin substitution and burn treatment. *Biomaterials* 2004;25(9):1559–67. [PubMed: 14697858]
3. Singer AJ, Berruti L, Thode HC Jr, McClain SA. Standardized burn model using a multiparametric histologic analysis of burn depth. *Acad Emerg Med* 2000;7(1):1–6. [PubMed: 10894235]
4. Singer AJ, McClain SA. A porcine burn model. *Methods Mol Med* 2003;78:107–19. [PubMed: 12825265]
5. Singer AJ, McClain SA. Development of a porcine excisional wound model. *Acad Emerg Med* 2003;10(10):1029–33. [PubMed: 14525733]
6. Sullivan TP, Eaglstein WH, Davis SC, Mertz P. The pig as a model for human wound healing. *Wound Repair Regen* 2001;9(2):66–76. [PubMed: 11350644]
7. Meyer W, Schwarz R, Neurand K. The skin of domestic mammals as a model for the human skin, with special reference to the domestic pig. *Curr Probl Dermatol* 1978;7:39–52. [PubMed: 752456]
8. Forbes, PD. Advances in the biology of skin Hair growth. Montagna, W.; Dobson, RL., editors. Vol. 9. Oxford: Pergamon; 1969. p. 419-32.
9. Heinrich W, Lange PM, Stirtz T, Iancu C, Heidemann E. Isolation and characterization of the large cyanogen bromide peptides from the alpha1- and alpha2-chains of pig skin collagen. *FEBS Lett* 1971;16(1):63–7. [PubMed: 11945902]
10. Gray GM, White RJ, Williams RH, Yardley HJ. Lipid composition of the superficial stratum corneum cells of pig epidermis. *Br J Dermatol* 1982;106(1):59–63. [PubMed: 7059505]
11. Wollina U, Berger U, Mahrle G. Immunohistochemistry of porcine skin. *Acta Histochem* 1991;90(1):87–91. [PubMed: 1710864]
12. Guide for the Care and Use of Laboratory Animals. Washington, D.C.: National Academy Press; 1996.
13. Seropian R, Reynolds BM. Wound infections after preoperative depilatory versus razor preparation. *Am J Surg* 1971;121(3):251–4. [PubMed: 5546329]
14. Harvey-Clark CJ, Giles K, Riggs KW. Transdermal fentanyl compared with parenteral buprenorphine in post-surgical pain in swine: a case study. *Lab Anim* 2000;34(4):386–98. [PubMed: 11072859]
15. Malavasi LM, Jensen-Waern M, Jacobson M, Ryden A, Ohagen P, Nyman G. Effects of extradural morphine on end-tidal isoflurane concentration and physiological variables in pigs undergoing abdominal surgery: a clinical study. *Vet Anaesth Analg* 2006;33(5):307–12. [PubMed: 16916353]

16. Malavasi LM, Nyman G, Augustsson H, Jacobson M, Jensen-Waern M. Effects of epidural morphine and transdermal fentanyl analgesia on physiology and behaviour after abdominal surgery in pigs. *Lab Anim* 2006;40(1):16–27. [PubMed: 16460586]
17. Malavasi LM, Augustsson H, Jensen-Waern M, Nyman G. The effect of transdermal delivery of fentanyl on activity in growing pigs. *Acta Vet Scand* 2005;46(3):149–57. [PubMed: 16261927]
18. Furst W, Banerjee A, Redl H. Comparison of structure, strength and cytocompatibility of a fibrin matrix supplemented either with tranexamic acid or aprotinin. *J Biomed Mater Res B Appl Biomater*. 2006
19. Swindle, MM. Swine in the laboratory: surgery, anesthesia, imaging, and experimental techniques. Vol. 2. Boca Raton, FL: CRC Press; 2007.
20. Singer AJ, Nable M, Cameau P, Singer DD, McClain SA. Evaluation of a new liquid occlusive dressing for excisional wounds. *Wound Repair Regen* 2003;11(3):181–7. [PubMed: 12753599]
21. Singer AJ, Thode HC Jr, McClain SA. Development of a histomorphologic scale to quantify cutaneous scars after burns. *Acad Emerg Med* 2000;7(10):1083–8. [PubMed: 11015238]
22. Mittermayr R, Wassermann E, Thurnher M, Simunek M, Redl H. Skin graft fixation by slow clotting fibrin sealant applied as a thin layer. *Burns* 2006;32(3):305–11. [PubMed: 16522355]
23. Nanney LB, Wenczak BA, Lynch JB. Progressive burn injury documented with vimentin immunostaining. *J Burn Care Rehabil* 1996;17(3):191–8. [PubMed: 8736363]
24. Winter GD. Formation of the scab and the rate of epithelization of superficial wounds in the skin of the young domestic pig. *Nature* 1962;193:293–4. [PubMed: 14007593]
25. Silverstein, P.; Goodwin, MN.; Raulston, GL.; Pruitt, B. The ultrastructure of collagen. Longrace, JJ., editor. Springfield, IL: Thomas; 1976.
26. Gallant CL, Olson ME, Hart DA. Molecular, histologic, and gross phenotype of skin wound healing in red Duroc pigs reveals an abnormal healing phenotype of hypercontracted, hyperpigmented scarring. *Wound Repair Regen* 2004;12(3):305–19. [PubMed: 15225209]
27. Liang Z, Engrav LH, Muangman P, Muffley LA, Zhu KQ, Carrougner GJ, et al. Nerve quantification in female red Duroc pig (FRDP) scar compared to human hypertrophic scar. *Burns* 2004;30(1):57–64. [PubMed: 14693087]
28. Xie Y, Zhu KQ, Deubner H, Emerson DA, Carrougner GJ, Gibran NS, et al. The microvasculature in cutaneous wound healing in the female red Duroc pig is similar to that in human hypertrophic scars and different from that in the female Yorkshire pig. *J Burn Care Res* 2007;28(3):500–6. [PubMed: 17438498]
29. Zhu KQ, Engrav LH, Gibran NS, Cole JK, Matsumura H, Piepkorn M, et al. The female, red Duroc pig as an animal model of hypertrophic scarring and the potential role of the cones of skin. *Burns* 2003;29(7):649–64. [PubMed: 14556722]
30. Thourani VH, Ingram WL, Feliciano DV. Factors affecting success of split-thickness skin grafts in the modern burn unit. *J Trauma* 2003;54(3):562–8. [PubMed: 12634539]





**Fig. 1.**

Custom-made aluminum burn application device. Application pressure is measured by a 50 ml syringe attached to the aluminum bar via the heat insulation unit. This device was designed to reach a pressure of  $0.4 \text{ kg/cm}^2$  when the piston is pushed into the barrel of the syringe from the "20 ml" mark down to the "10 ml" mark with one hand, while the other hand keeps the unit in place without exerting additional pressure.

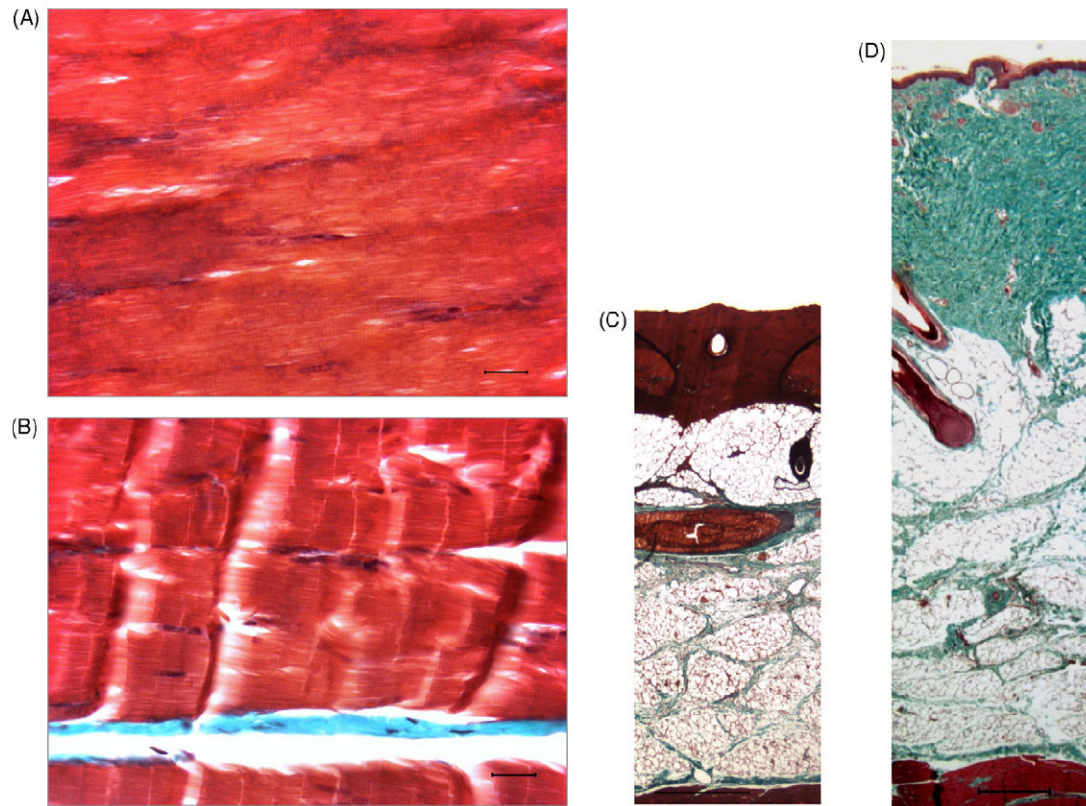


**Fig. 2.**

(A) Skeletal muscle from wound ground 24 h after burn and (B) skeletal muscle from wound ground without preceding burn. Muscle fasciculi cut longitudinally. After burn injury, the structure with wider endomysium, containing loose collagenous connective tissue (stained blue), changes to a more compact structure, however, no coagulation or necrosis of the muscle fibres is noted. Masson's trichrome, 400 $\times$  magnification. Bar represents 20  $\mu$ m. (C) Dermal and subdermal tissue 24 h after burn and (D) healthy dermal and subdermal tissue. Loss of viable tissue represented by color change from green (healthy connective tissue) to red (coagulated tissue). A general compression of tissue thickness is observed. Masson's trichrome, 25 $\times$  magnification. Bar represents 600  $\mu$ m. (For interpretation of the references to color in this figure legend, the reader is referred to the web version of the article.)



**Fig. 3.** Multi-layer dressing to ensure maximum protection against outside contamination and avoid cross-contamination of wound fields when different test substances are used on adjacent wound fields.



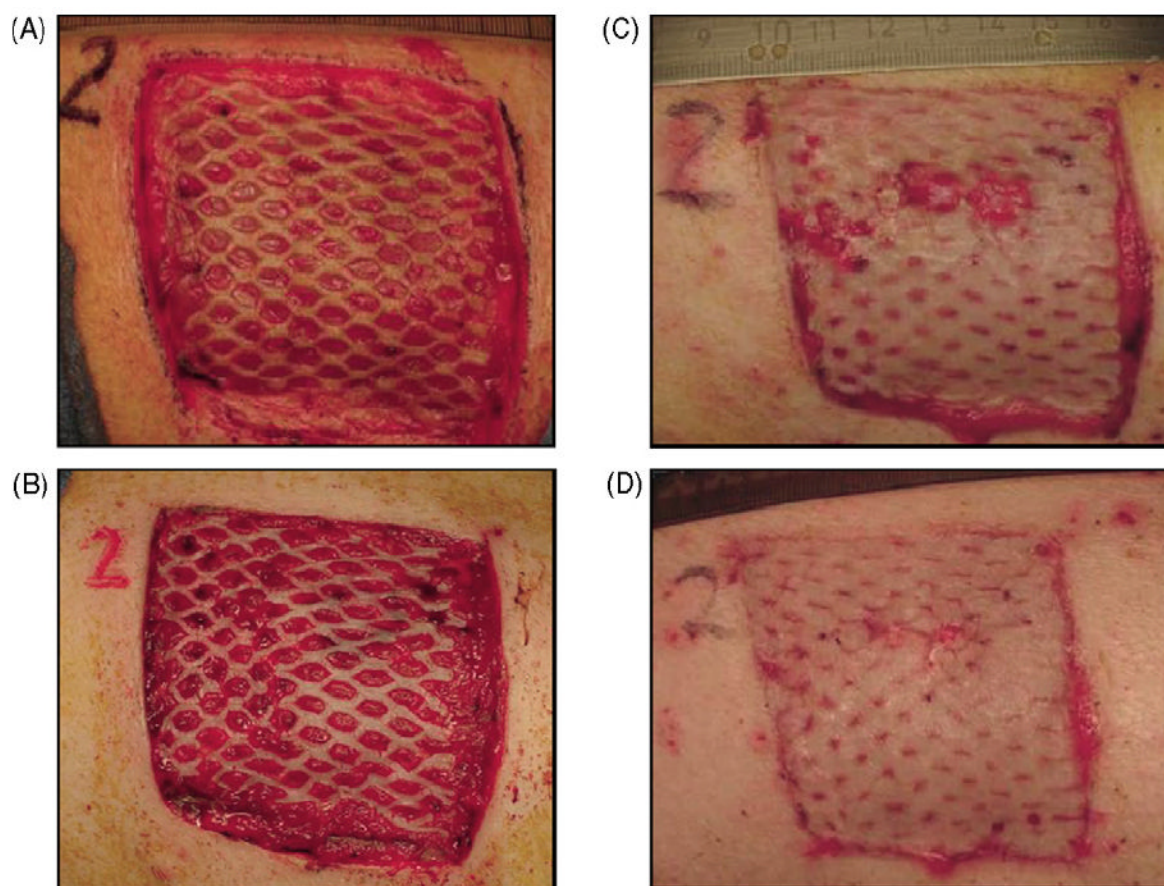


**Fig. 4.**  
Digital photographs of a wound series showing wound closure during the course of the study.  
(A) Postoperative (PO) day 0. (B) PO day 5. (C) PO day 9. (D) PO day 14.

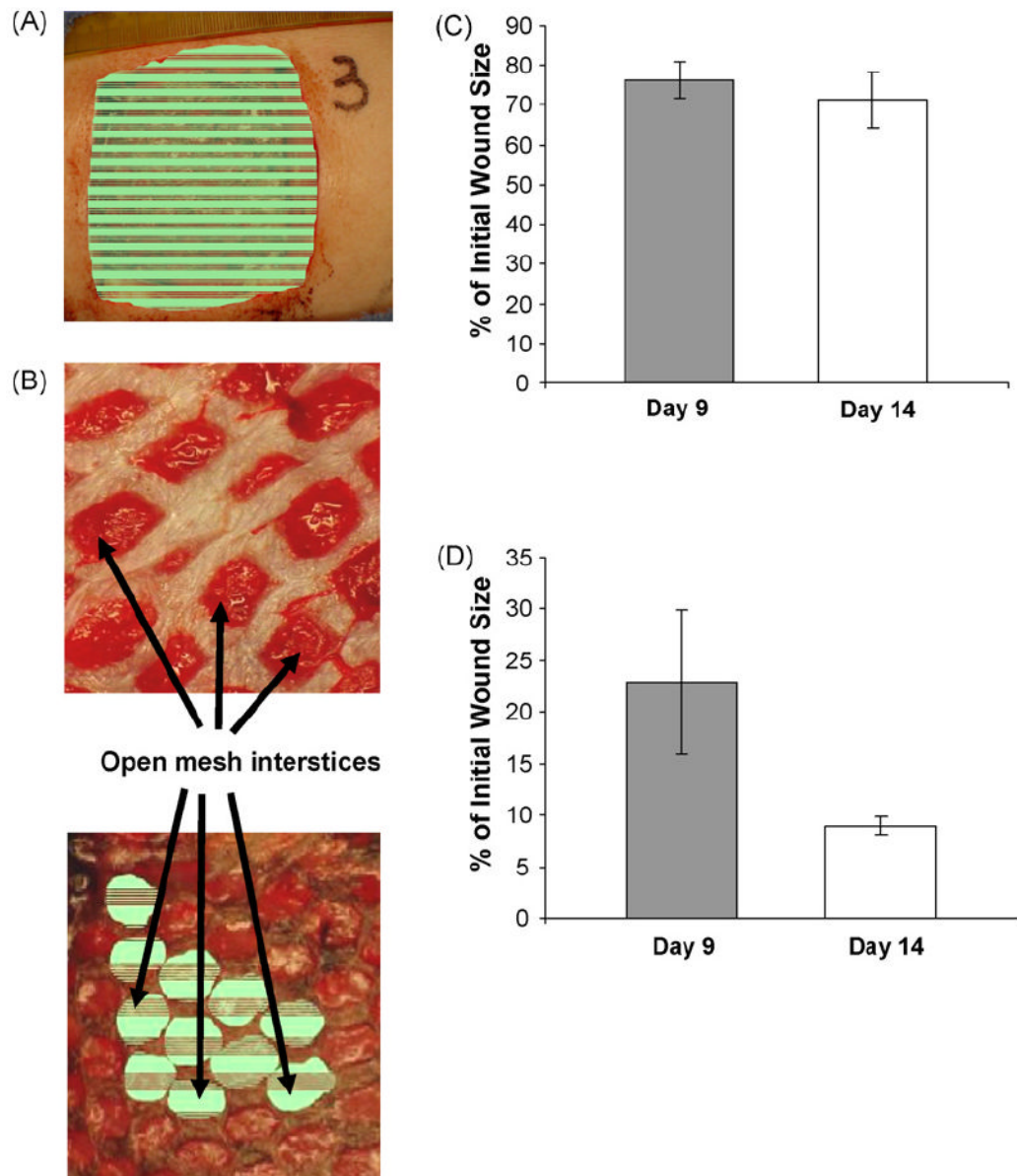


**Fig. 5.**

Planimetric wound measurements. (A) Entire burn size traced and measured by planimetry using computer software. (B) Autograft mesh interstices are manually and individually traced. The total wound size is measured by planimetry. (C) Wounds show a contraction of approximately 25% of the initial wound size throughout a typical experimental course. (D) Open wound size in % of original wound size at days 9 and 14 post autograft coverage. Data presented as means  $\pm$  standard error of the mean,  $n = 8$ .

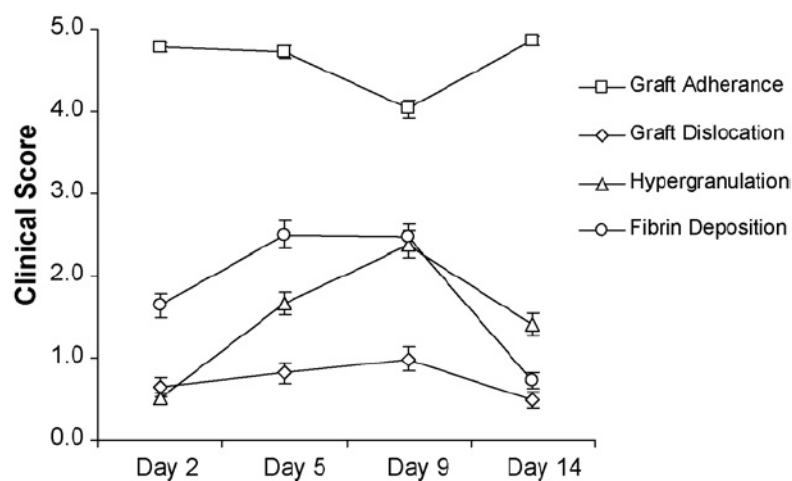


**Fig. 6.** Clinical assessment scores for graft adherence, graft dislocation, hypergranulation, and fibrin deposition in a series of control wound fields at postoperative days 2, 5, 9 and 14. Clinical scores were made according to Table 1. Data presented as means  $\pm$  standard error of the mean,  $n = 11$ .



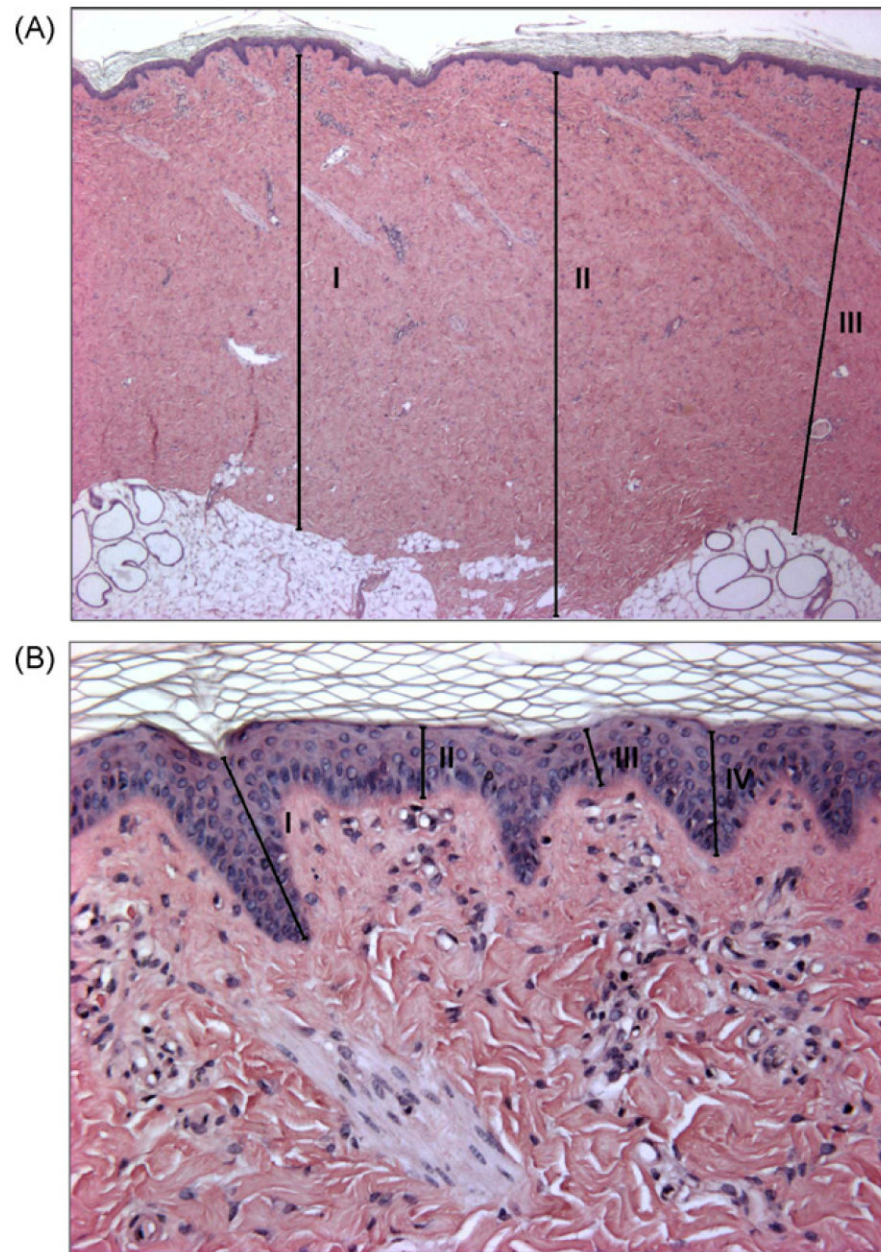


**Fig. 7.** Cross section of wound center at postoperative day 14. Hematoxylin and Eosin staining. (A) Dermal tissue with three measurement markings (I = 2370  $\mu\text{m}$ , II = 2735  $\mu\text{m}$ , III = 2254  $\mu\text{m}$ , 25 $\times$  magnification). (B) Epidermal tissue with four measurement markings (I = 124  $\mu\text{m}$ , II = 44  $\mu\text{m}$ , III = 36  $\mu\text{m}$ , IV = 76  $\mu\text{m}$ , 200 $\times$  magnification).

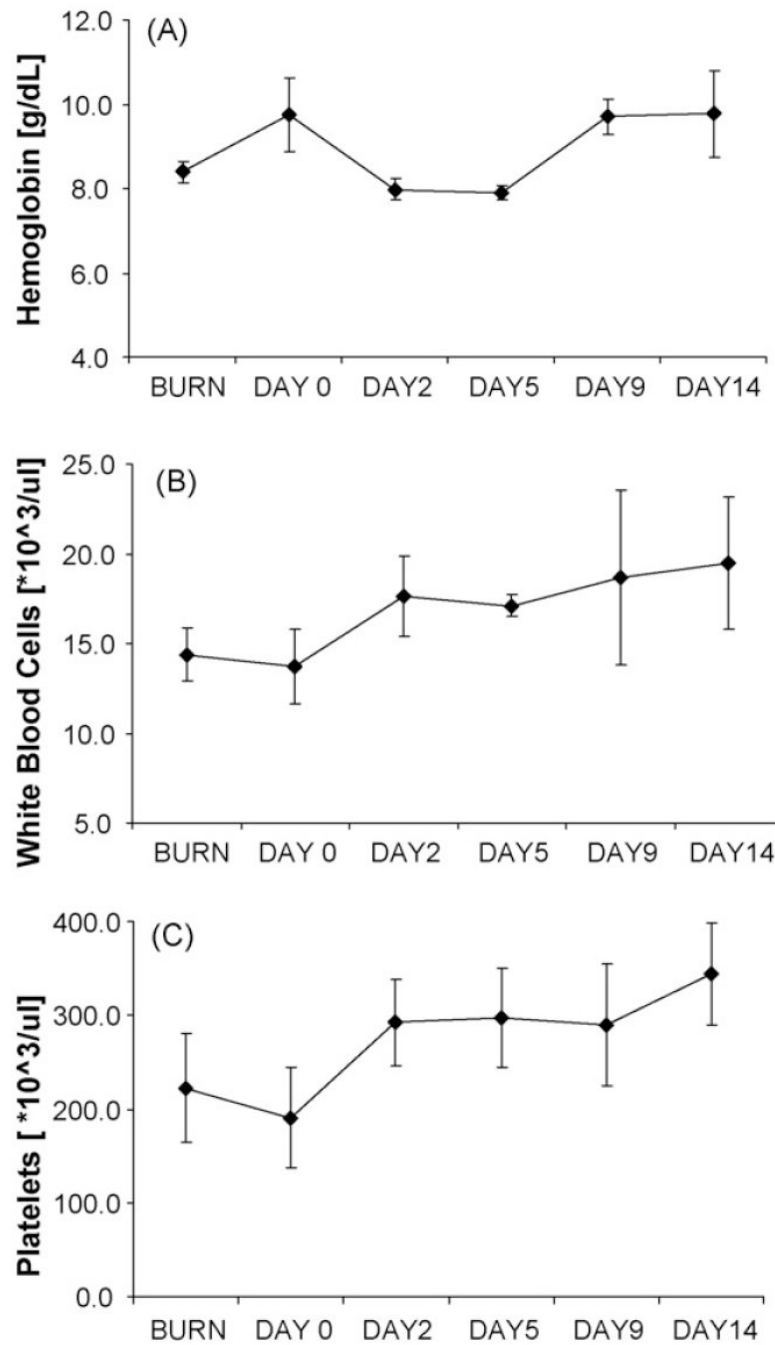


**Fig. 8.** Mean levels for (A) hemoglobin, (B) white blood cells, and (C) platelets. No pathologically elevated values were detected. Data presented as means  $\pm$  standard error of the mean,  $n = 6$ .

Table 1

Clinical wound assessment scores

Grade	Graft dislocation	Graft adherence	Granulation tissue	Hyper granulation	Hematoma	Fibrin deposition
0	None	Full graft loss	None; full depth defect	None	None	None
1	5–10%, tissue still fully viable	Graft 20% adherent, 50% graft loss	Low level of granulation tissue	10%	Up to 10% wound size	Small patches, up to 10% wound size
2	10–25%, one or two spots, 10% tissue not viable	Graft 50% adherent, 30% graft loss	Granulation tissue level at half of initial wound depth	20%	Up to 20% wound size	Thicker, confluent patches, up to 20% wound size
3	25–50%, more than 20% tissue not viable	Graft 75% adherent, 20% graft loss	Granulation tissue level just below surrounding tissue	40%	Up to 40% wound size	Up to 40% wound size
4	50–80%, more than 50% tissue not viable	Graft 90% adherent	Granulation at level with surrounding tissue	65%	Up to 60% wound size, partial graft loss	Up to 60% wound size, partial graft loss
5	Graft completely dislocated, full tissue loss	Full graft adherence	Fully granulated wound, exceeds level of surrounding tissue	100%	Up to 100% total graft loss	Wound fully covered with fibrin and graft skin totally macerated